Fottea, 26(1), 29–39, 2026
doi: 10.5507/fot.2025.012

Czech Phycological Society

Parabrasilonema hainanensis gen. et sp. nov. (Scytonemataceae, Nostocales), a novel filamentous cyanobacterium isolated from a tropical reservoir in China

Qi Zhang[1,2], Lin Li[3], Tianli Li[2], Lingling Zheng[2] and Lirong Song[2]

Abstract

A filamentous, heterocytous cyanobacterial strain FACHB–3638 was isolated from Yongzhuang Reservoir, a tropical drinking water reservoir on Hainan Island, southern China. This cyanobacterium formed macroscopic, felt–like mats on submerged concrete substrates, covering extensive areas of the shallow riverbed. The filaments were isopolar, cylindrical, and nearly straight or flexuous, exhibiting infrequent scytonematoid false–branching and producing firm, often layered and colored sheaths. Morphologically, the strain resembles members of the Scytonemataceae family, particularly *Brasilonema*, but phenotypically differed from other scytonematoid genera in thallus form, branching pattern, trichome structure, heterocyte positioning, and habitat preference. Phylogenetic analyses based on 16S rRNA gene sequences placed this strain in a clade distinct from closely related genera within the family Scytonemataceae. The 16S rRNA sequence of this strain shared less than 95% genetic identity with currently described Scytonemataceae genera. Based on a polyphasic approach including data on morphology, ultrastructure, ecology, 16S rRNA phylogeny and secondary structure, we propose *Parabrasilonema hainanensis gen. et sp. nov.* as a new cyanobacterial taxon. Additionally, phylogenetic analyses showed that strain FACHB–3638, along with uncultured cyanobacteria clone Z32 from wall biomats in a deep sinkhole in northeastern Mexico, forms a well–supported monophyletic clade, exhibiting 97.51–99.28% nucleotide similarity. These findings suggest that these uncultured cyanobacteria likely belong to the genus *Parabrasilonema*, broadening our understanding of its diversity across distinct habitats.

Keywords

Cyanobacteria; New genus; *Parabrasilonema*, Polyphasic approach; Taxonomy; Yongzhuang Reservoir

[1]*Key Laboratory of Lake and Watershed Science for Water Security, Institute of Hydrobiology, Chinese Academy of Sciences, Wuhan 430072, China*;
[2]*National Aquatic Biological Resource Center, Institute of Hydrobiology, Chinese Academy of Sciences, Wuhan 430072, China*
[3]*Key Laboratory of Algal Biology, Institute of Hydrobiology, Chinese Academy of Sciences, Wuhan 430072, China*

Corresponding author
Lirong Song
lrsong@ihb.ac.cn

Article History
Received March 26, 2025
Revised June 23, 2025
Accepted October 6, 2025
Published online March 31, 2026

Supplementary Material
None

How to cite
Zhang, Q., Li, L.,Li, T., Zheng, L., & Song, L. (2026). *Parabrasilonema hainanensis gen. et sp. nov.* (Scytonemataceae, Nostocales), a novel filamentous cyanobacterium isolated from a tropical reservoir in China. *Fottea*, *26*(1), 29–39. https://doi.org/10.5507/fot.2025.012

Introduction

Cyanobacteria, oxygenic photosynthetic prokaryotes containing chlorophyll-*a* and phycobiliproteins, are highly adaptable and occupy diverse habitats across the planet (Castenholz & Waterbury, 1989; Whitton & Potts, 2012). Filamentous cyanobacteria are particularly prevalent in aquatic environments, often forming prominent components of attached communities in submerged habitats within both standing and flowing waters (Komárek & Johansen, 2015). Historically, cyanobacteria have been classified primarily based on morphological characteristics (Geitler, 1932; Komárek, 2013). However, this traditional taxonomy, reliant on morphological criteria, often struggles to accurately reflect evolutionary relationships (Komárek *et al*., 2014). The polyphasic approach, integrating morphological, molecular, physiological, cytological and ecological data, has recently been considered as a powerful tool for resolving controversies in cyanobacterial taxonomy and

systematics, and it is essential for describing new taxa (Mareš, 2017; Barbosa *et al*., 2021).

The order Nostocales within the phylum Cyanobacteria represents a large monophyletic group of filamentous cyanobacteria, consisting of thalli with unbranched and isopolar, and falsely or true branched types containing specialized cells such as heterocytes and akinetes (Komárek *et al*., 2014; Kumar *et al*., 2023). According to modern phylogenetic and combined polyphasic assessment, Strunecký *et al*. (2023) systematically classified Nostocales into 13 families: Aphanizomenonaceae, Capsosiraceae, Geitleriaceae, Hapalosiphonaceae, Heteroscytonemataceae, Leptobasaceae, Nodulariaceae, Nostocaceae, Rhizonemataceae, Rivulariaceae, Scytonemataceae, Stigonemataceae and Tolypothrichaceae. Modern phylogenetic and combined polyphasic analyses have confirmed that the family Scytonemataceae is well–defined and clearly distinguishable (Fiore *et al*., 2007; Komárková *et al*., 2013). Komárek *et al*. (2014) characterized Scytonemataceae as an isopolar, false–branching heterocytous family, comprising six genera: the type genus *Scytonema* Agardh, Bornet *et* Flahault, as well as *Brasilonema* Fiore, Sant–Anna, de Paiva Azevedo, Komárek, Kaštovský, Sulek *et* Lorenzi, *Chakia* Komárková, Zapomělová *et* Komárek, *Iphinoe* Lamprinou *et* Pantazidou, *Petalonema* Berkeley *et* Wolle and *Symphyonemopsis* Tiwari *et* Mitra. Recent studies have described additional genera, such as *Aetokthonos* Wilde *et* Johansen, *Ewamiania* McGregor *et* Sendall, *Iningainema* McGregor *et* Sendall, and *Spelaeonaias* Lamprinou, Christodoulou, Hernández–Mariné *et* Economou–Amilli, highlighting the increasing diversity within this family (Lamprinou *et al*., 2016; McGregor & Sendall, 2017a, b; Wilde *et al*., 2014). *Brasilonema* was originally isolated and described from Brazil, having been separated from *Scytonema* based on morphological and phylogenetic distinctions, particularly its formation of fascicles and rare false branching (Fiore *et al*., 2007). Bohunická *et al.* (2024) conducted a comprehensive survey of *Brasilonema* strains across North, Central, and South America, Central Africa, South and East Asia, and Europe. They reported the discovery of 24 new species and provided evidence that *Brasilonema* exhibits a clear ecological preference for subaerial and terrestrial habitats, being widely distributed in tropical and subtropical regions with humid climates. Since its original description, more than forty species have been identified, including both newly described taxa and reassignments of previously known species from other genera.

Hainan Island, located at the northern fringe of the Oriental tropics, is separated from the Chinese mainland by the Qiongzhou Strait. Yongzhuang Reservoir, situated in Haikou City, Hainan Province, serves as a drinking water source, spanning an area of 6.03 km² with a total storage capacity of 10.15 million m³ and a daily supply capacity of up to 100,000 m³ (Zhang *et al*., 2023). This tropical reservoir exhibits eutrophic conditions during the flooding season (May to October), and transitions to mesotrophic conditions during the dry season (November to April). Over the past decade, filamentous cyanobacteria such as *Pseudanabaena* sp. and *Limnothrix* sp. have dominated the phytoplankton community during the flooding season (Gao *et al*., 2013). To investigate the diversity of algal populations in Yongzhuang Reservoir in 2021, we identified and isolated dominant species *Planktothricoides raciborskii* (Woloszyńska) Suda *et* Watanabe, *Pseudanabaena* sp., *Raphidiopsis raciborskii* (Woloszyńska) Aguilera, Berrendero Gómez, Kaštovský, Echenique *et* Salerno and *Limnothrix planktonica* (Woloszyńska) Meffert from water samples. Thick biomats, primarily composed of filamentous cyanobacteria, covered the concrete substrates of shallow river inlets for most of the year.

In this study, we describe a novel filamentous cyanobacterial taxon isolated from biomats in Yongzhuang Reservoir. This taxon represents a significant component of attached communities in submerged, flowing water habitats. Taxonomic assignment has been determined through a comprehensive polyphasic approach including morphology, ecology, 16S rRNA phylogeny, and secondary structures of the 16S–23S ITS region.

Materials and Methods

Sampling, isolation and cultivation: Samples were collected from algal mats attached to submerged concrete substrata near the inlet of Yongzhuang Reservoir (19°58′5.7″ N, 110°15′41.9″ E) on 3 July 2021. Monoclonal isolates were obtained by micropipetting individual filaments or hormogonia under an inverted microscope Olympus CKX 41 (Tokyo, Japan) and transferring them to microtitration plates (24 wells) containing liquid BG11 medium (Stanier *et al*., 1971; Zhang *et al*., 2024). All unialgal isolates were cultivated on standard BG11 medium and BG11 without nitrogen at 22 °C under a light–dark cycle with illumination of 20 $\mu mol \cdot m^{-2} \cdot s^{-1}$. An isolated strain was deposited in the Freshwater Algae Culture Collection at the Institute of Hydrobiology (FACHB), National Aquatic Biological Resource Center, Institute of Hydrobiology, Chinese Academy of Sciences, as a perpetually transferred culture.

Light and transmission electron microscopy: Morphological observations were conducted using a light microscope Olympus BX 53 (Tokyo, Japan) with differential interference contrast. High–resolution images were captured using an Olympus DP80 camera and Olympus cellSens Standard software. Microscopic images were taken during the exponential phase (1–3 months after transfer) and the stationary phase (4–6 months after transfer) (Mai *et al*., 2018). Morphological characteristics, including filament and trichome diameter, thallus and sheath morphology, cell color and content, heterocyte dimensions, branching, and hormogonia development, were measured and compared (Barbosa *et al*., 2021). A total of 110 measurements were performed to determine cell width and length.

Cellular ultrastructure was examined using transmission electron microscopy (TEM). Cyanobacterial cells were fixed with 2.5% glutaraldehyde in 0.1 M phosphate buffer (pH 7.2) at 4 °C. After washing with 0.1 M phosphate buffer (pH 7.2) three times, samples were post–fixed with 2% osmium tetroxide in the same buffer for 2 hours. The fixed material was

dehydrated in a graded ethanol series at 4 °C and embedded in Spurr's resin via propylene oxide (Spurr 1969). Ultrathin sections were post–stained with 1% uranyl acetate solution and 1% lead citrate, and examined in a Hitachi HT–7700 transmission electron microscope (Tokyo, Japan) at an accelerating voltage of 80 kV.

DNA extraction, amplification and sequencing: Unialgal cultures were harvested, and total genomic DNA was extracted from approximately 100 mg of fresh biomass using a NuClean Plant Genomic DNA Kit (CWBIO; Taizhou, China) following the manufacturer's protocol. The 16S rRNA gene and the 16S–23S ITS region was amplified using the primer sets CYA106F/23S5′R (Baurain *et al*., 2002; Nübel *et al*., 1997) and F322/R340 (Iteman *et al*., 2000). Each reaction was prepared in a 50 µL volume as described in Zhang *et al*. (2024). Polymerase chain reactions (PCR) were performed in a BioRad PCR Thermocycler T100 (Bio–Rad Laboratories, Inc., USA) with the following conditions: an initial denaturation step at 94 °C for 2 min, followed by 35 cycles of 94 °C for 40 s, annealing at 55 °C for 40 s, extension at 72 °C for 1.5 min, and a final extension step at 72 °C for 4 min. Sequencing was carried out using an ABI 3700 sequencer (Applied Biosystems; California, USA). Sequences obtained from both DNA strands were manually checked after automatic assembly using Chromas PRO.

Phylogenetic analyses: 16S rRNA gene sequences obtained in this study and reference sequences retrieved from GenBank using BLAST were aligned using Clustal W (Larkin *et al*., 2007). Phylogenetic trees were constructed using maximum likelihood (ML) and Bayesian (BI) methods. Evolutionary models for ML and BI analyses were determined using jModelTest v. 2.1.5 based on the Akaike information criterion (AIC) (Darriba *et al*., 2012). The best–fit evolutionary model for the 16S rRNA gene was GTR + I + G. ML analyses were performed with 1,000 bootstrap replicates using MEGA X software (Kumar et al. 2018), and bootstrap percentages (BP) were calculated. BI analyses were conducted using MrBayes v. 3.2.2 (Ronquist *et al*., 2012) with two runs of six Markov chain Monte Carlo executed for 5×10^6 generations, sampling every 100 generations, and a burn–in of 25%. The final average standard deviation of split frequencies was < 0.01, and Bayesian posterior probabilities (PP) were calculated. Uncorrected *p*–distance for 16S rRNA sequences were calculated using MEGA X to determine sequence similarity (100 × (1-*p*)). Secondary structures of the 16S–23S ITS region, including helices D1–D1′, Box–B and V3 helices, were predicted using the Mfold web server (Zuker, 2003) with default parameters and re–drawn using Adobe Illustrator CS5 (Adobe Systems Incorporated, California, USA).

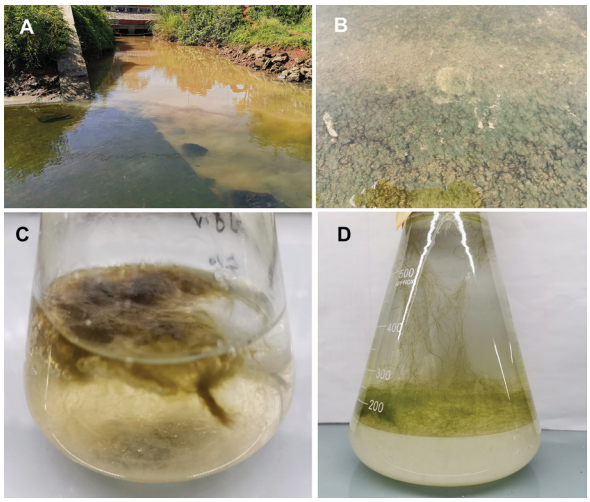

Fig. 1. Colonies of *Parabrasilonema hainanensis* from Yongzhuang Reservoir **(A, B)** and in culture **(C, D)**.

Results

Morphology

The tropical cyanobacterial strain isolated from Reservoir Yongzhuang was identified as a dominant component of attached communities on submerged concrete substrata in flowing streams near the reservoir's inlet (Fig. 1A, B). The entire shallow riverbed was covered with mats primarily composed of this filamentous cyanobacterium. Filaments were often attached to agar substrates and formed macroscopic mats, and occasionally free–floating in culture (Fig. 1C, D). Motility of the filaments was not observed. Cells were discoid or cylindrical, olive green, yellow–green or yellow–brown, measuring 0.3 to 1.0 × longer than wide. The ratio between length and diameter was usually decreased in older trichomes (Fig. 2A–H). Cell content often appeared conspicuously granular in the centroplasm, with visible chromatoplasm (Fig. 2B). Rows of cells occasionally contained large, solitary, central vacuole–like structures (Fig. 2C). Apical cells were rounded or obtuse–conical, occasionally with vacuole–like structures (Fig. 2 D, E). The sheath thickened with age, sometimes becoming lamellated and dark gray (Fig. 2F–H). Necridic cells were observed, lyophilizing to leave dark pigment residues between cells within the sheath (Fig. 2I). Filaments were rarely *Scytonema*–like false branched (Fig. 2J–L). Heterocytes were infrequent, intercalary, light yellow, occurring singly or in pairs, and varied in shape from discoid to cylindrical (Fig. 2M). Cell shape and arrangement often became irregular in meristematic zones (Fig. 2N). Reproduction occurred through fragmentation of trichomes and the formation of hormogonia. The hormogonia were short, released from the ends of the filaments, and sometimes contained granules and vacuole–like structures (Fig. 2O–Q).

TEM revealed a persistent sheath typically comprising four fibrillar layers parallel to the long axis of the filament, separated from the cell wall by a thick transparent zone (Fig. 3). Cell constrictions were shallow and occasionally wavy in longitudinal section (Fig. 3A–C). Cell division was symmetrical and perpendicular to the long axis of the trichome (Fig. 3B, C). Thylakoids were irregularly distributed over the cell volume, often agglomerated near the periphery (Fig. 3C, D). One to several carboxysomes were usually present in centroplasm (Fig. 3E).

Molecular and phylogenetic analyses

Phylogenetic trees based on 16S rRNA gene, constructed using an alignment of 191 representative taxa comprising 1,182 nucleotides, were inferred through maximum

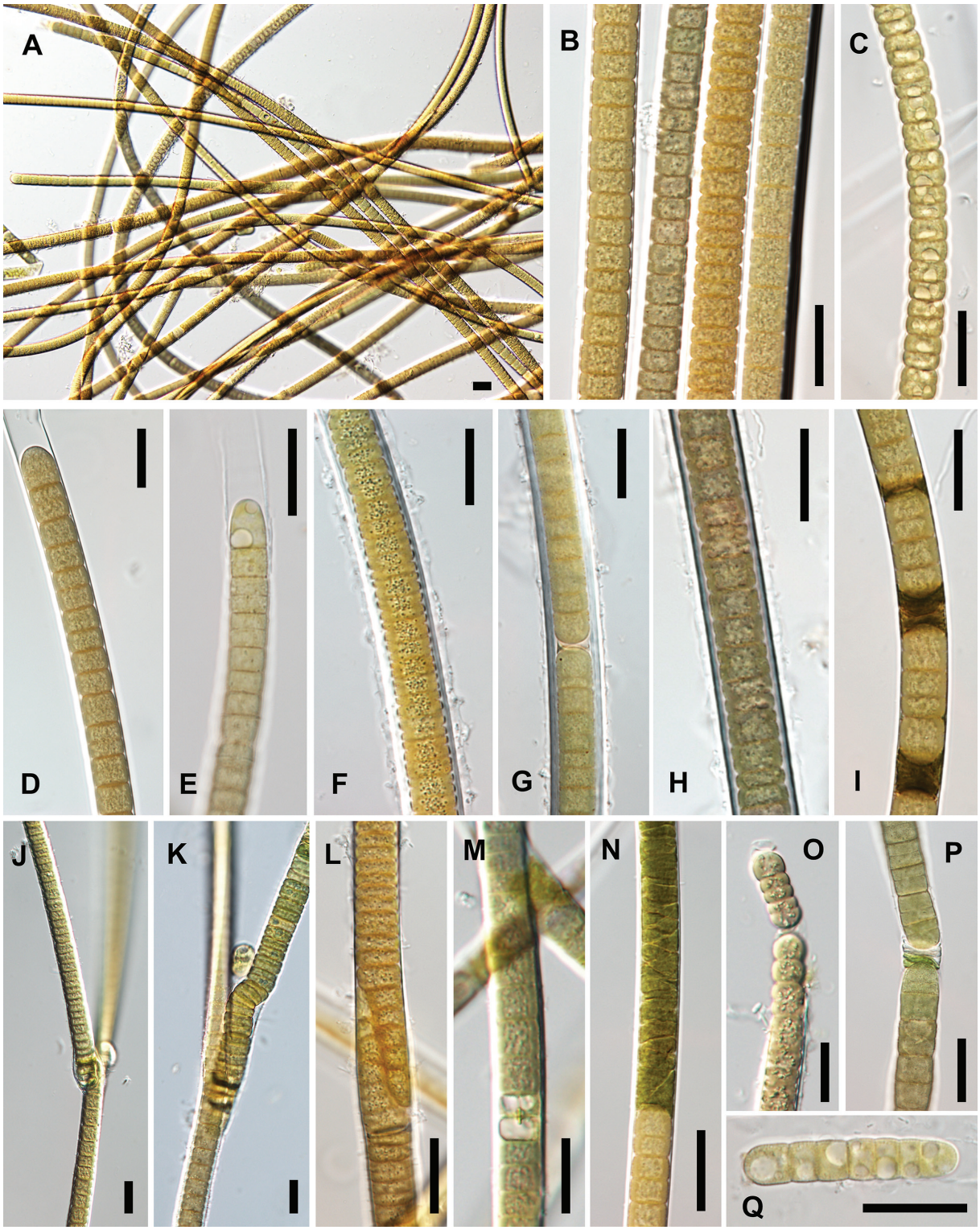

Fig. 2. Light micrographs of *Parabrasilonema hainanensis* (reference strain FACHB–3638). **(A)** Straight or curved filaments from monospecific cultures. **(B)** Filaments at different growth stages. **(C)** Rows of cells containing large central vacuole–like structures. **(D, E)** Filaments with rounded or obtuse–conical apical cells. **(F–H)** Older filaments showing gradually thickening sheaths. **(I)** Dark necridia abundant in mature trichome. **(J, K)** False branching. **(L)** Formation of false branch. **(M)** Intercalary heterocytes. **(N)** Rapid cell division in meristematic zone. **(O, P)** Hormogonia formation. **(Q)** Short hormogonia with prominent vacuolization. Scale bars 20 μm.

likelihood (ML) and Bayesian inference (BI) methods. The ML phylogenetic tree, with Bayesian posterior probabilities indicated, was shown in Fig. 4. Strain FACHB–3638, along with some uncultured cyanobacteria, formed a distinct clade with strong support. This clade exhibited a close relationship with a cluster comprising sequences from *Brasilonema*, *Ewamiania*, *Iphinoe*, *Petalonema*, *Scytonema* and *Symphyonemopsis* within

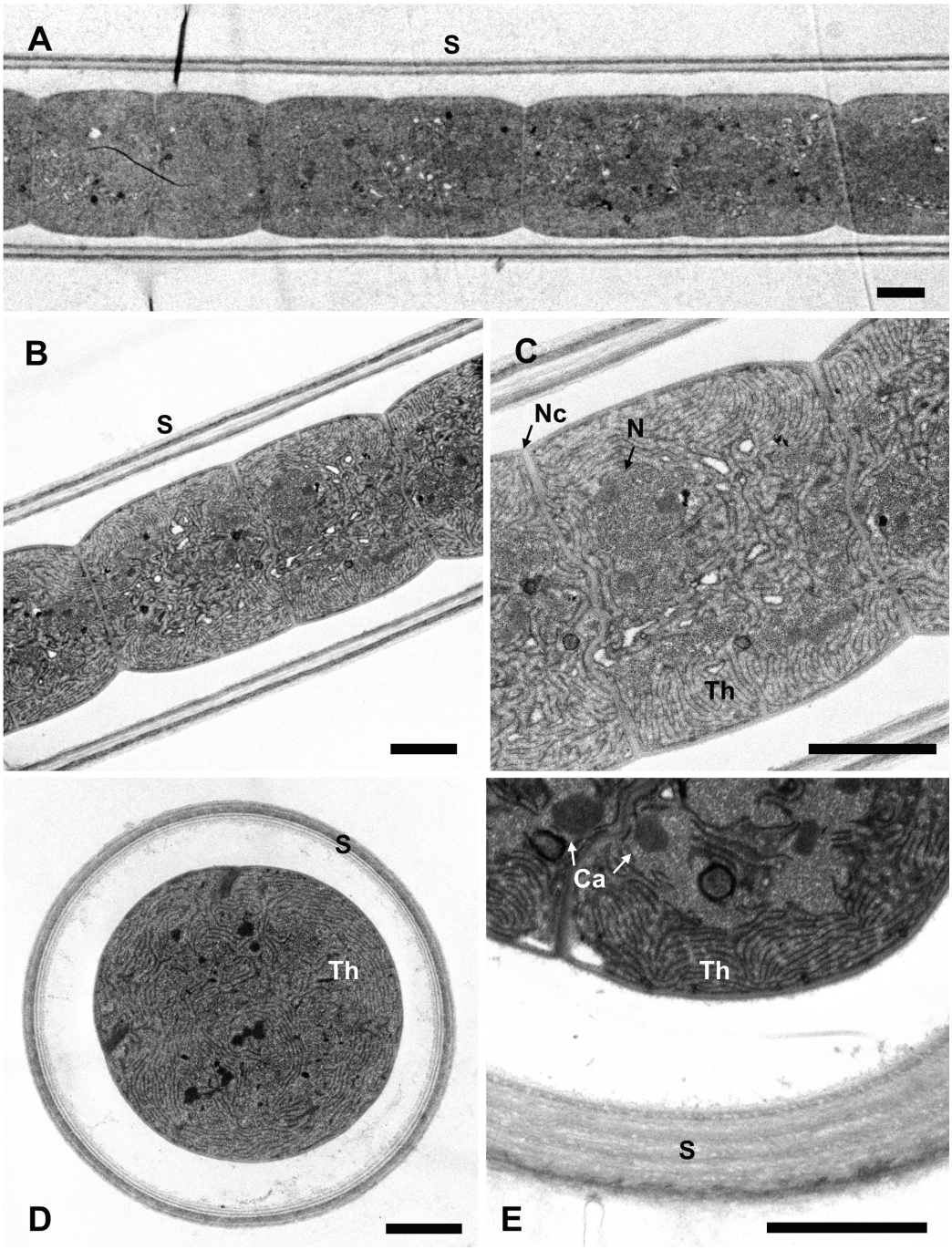

Fig. 3. Transmission electron micrographs of *Parabrasilonema hainanensis* (reference strain FACHB–3638). **(A, B)** Section of cylindrical cell in longitudinal view, showing stratified sheath (S). **(C)** Section of cylindrical cell in longitudinal view, showing nucleoplasmic region (N), new cross–wall formation (Nc) and thylakoids (Th). **(D)** Section of cell in cross–section, showing sheath (S) and thylakoids (Th). **(E)** Section of cell in cross–section, showing carboxysomes (Ca), stratified sheath (S) and thylakoids (Th). Scale bars 2 μm.

the family Scytonemataceae. However, the isolate clearly diverged from other Scytonemataceae genera. Strain FACHB–3638 exhibited less than 94.5% 16S rRNA gene sequence similarities with representative strains of the genera, including *Cronbergia* (93.89%), *Brasilonema* (93.13–93.83%), *Symphyonemopsis* (93.56%), *Iphinoe* (92.97%), *Aetokthonos* (92.39%), *Ewamiania* (92.35%), *Chakia* (92.04%), *Petalonema* (91.96%) and *Scytonema* (91.20–92.98%) (Table 1). However, 16S rRNA sequences from uncultured cyanobacteria clone Z32 showed high similarities of 97.51–99.28% with FACHB–3638 (Table 1).

Secondary structure analysis of 16S–23S ITS region

The D1–D1′ helix consisted of 63 nucleotides, with basal bilateral bulge at position 6–7/52–58, a small asymmetrical bilateral bulge in the middle portion, and terminal loop (5′–AAAAGUAGA–3′) (Fig. 5). The Box–B helix contained 37 nucleotides, bearing a small basal bilateral bulge at position 5/32–33 and a large terminal loop (5′–GCCACAAAACAA–3′) (Fig. 6). The V3 helix

consisted of 43 nucleotides, with one basal unpaired adenine residue at position 40, a bilateral bulge in the middle portion at position 12–14/28–31 and terminal loop (5′–UAAAA–3′) (Fig. 6). These structures exhibited distinct differences compared to those of related taxa. These results indicate that we have a new genus of cyanobacterium which we now propose:

***Parabrasilonema* Q. Zhang *et* L. Song *gen. nov.* (Figs. 1–2)**

Description: Thallus attached to solid substrates, forming macroscopic colonies or mats. Filaments isopolar, solitary, long, nearly straight or flexuous, with false branching. Sheath firm, colorless or dark grey, thin or thick, sometimes lamellated, with one trichome per sheath. Trichomes isopolar, cylindrical, constricted at the cross walls, not attenuated towards the ends. Cells mostly shorter than wide, rarely isodiametric, without aerotopes, sometimes with granules and vacuole–like structures in cytoplasm. Apical cells rounded or obtuse–conical, without calyptra. Heterocytes intercalary, discoid up to cylindrical. Akinetes absent. Hormogonia and necridia present.

Etymology: The genus name refers to the cyanobacterium morphologically similar to *Brasilonema*. The prefix "*para–*" is derived from the Greek *pará*, which means near or beside.

Type species: *Parabrasilonema hainanensis* Q. Zhang *et* L. Song

***Parabrasilonema hainanensis* Q. Zhang *et* L. Song *sp. nov.* (Figs 1–2)**

Description: Thallus olive green, yellow–green and yellow–brown, attached to solid substrates, tuft–like spreading, and forming macroscopic feltlike mats (up to 5 cm high). Filaments long, nearly straight or flexuous, sometimes forming fascicles of trichomes, rarely scytonematoid false branched, 8.0–18.1 μm wide. Sheath firm, colorless, firstly thin, becoming thick with age, up to 4.7 μm wide, sometimes lamellated and dark grey. Trichomes isopolar, cylindrical, slightly to distinctly constricted at the cross walls, not attenuated towards the ends, with meristematic zones, 7.5–12.4 μm wide. Cells cylindrical to disc–like, mostly shorter than wide, rarely isodiametric, sometimes with granules and vacuole–like structures in cytoplasm, 3.0–9.5 μm long. Apical cells rounded or obtuse–conical, sometimes with vacuole–like structures, without calyptra. Heterocytes infrequent, intercalary, discoid up to cylindrical, 8.5–12.4 μm wide × 5.0–6.8 μm long. Necridic cells of dark color present, lyophilizing to leave dark pigment between cells within the sheath. Hormogonia short, typically 4–16 celled, released from the ends of the filaments, sometimes with granules and vacuole–like structures, 7.6–11.5 μm wide. Akinetes absent.

Holotype: HBI! Dried specimen (HN20210713) from reference strain FACHB–3638 deposited in Freshwater Algal Herbarium (HBI), Institute of Hydrobiology, Chinese Academy of Sciences, Wuhan, Hubei, China.

Type locality: Yongzhuang Reservoir (19°58'5.7" N, 110°15'41.9" E), Haikou, Hainan Province, China.

Habitat: Growing on submerged concrete substrates in flowing streams.

Etymology: The species epithet '*hainanensis*' refers to type locality, Hainan Island.

Reference strain: Strain FACHB–3638 deposited in Freshwater Algae Culture Collection at the Institute of Hydrobiology (FACHB–collection), National Aquatic Biological Resource Center, Wuhan, Hubei, China.

GenBank accession number: PQ858247, including partial 16S rRNA gene, 16S–23S ITS region and partial 23S rRNA gene; PQ862904, including partial *nifH* gene sequences.

Discussion

Genera are ideally defined as monophyletic clades with distinct morphological traits, necessitating phylogenetic analysis for genus–level identification (Mai *et al*., 2018). The 16S rRNA gene phylogeny supports the placement of our new isolate, *Parabrasilonema*, as a distinct genus within the family Scytonemataceae. Our phylogenetic analyses indicate that *Parabrasilonema* forms a subcade sister to other genera in Scytonemataceae. Most bacteriologists suggest a threshold for sequence identity of 16S rRNA below 94.5% to separate taxa into different genera, although this criterion is not absolute for separation of cyanobacterial genera (Mai *et al*., 2018; Yarza *et al*., 2014). In our study, the 16S rRNA gene sequence identity between *Parabrasilonema* and closely related taxa ranged from 91.20% to 93.89%. The unique secondary structures in D1–D1', Box–B and V3 helices of strain FACHB–3638 further confirm that this strain does not belong to any known related genera. The polyphasic approach, including data on morphology, ultrastructure, ecology, 16S rRNA phylogeny and secondary structure of the 16S–23S ITS region, provides comprehensive support for proposing *Parabrasilonema* as a new genus within Scytonemataceae.

The species–rich family Scytonemataceae is characterized by a complex thallus, typically with heterocytes and isopolar filaments exhibiting false branching (Komárek *et al*., 2014; Komárková *et al*., 2013). Morphologically, *Parabrasilonema* can be distinguished from other genera in Scytonemataceae based on branching patterns, trichome structure and the position of heterocytes, despite considerable morphological variability in filaments and trichomes (Komárková *et al*., 2013). The genus *Iphinoe* is unique within Scytonemataceae due to its exclusive true branching, primarily of the T–type (Lamprinou *et al*., 2011). *Petalonema* is characterized by solitary or small–grouped heteropolar filaments with

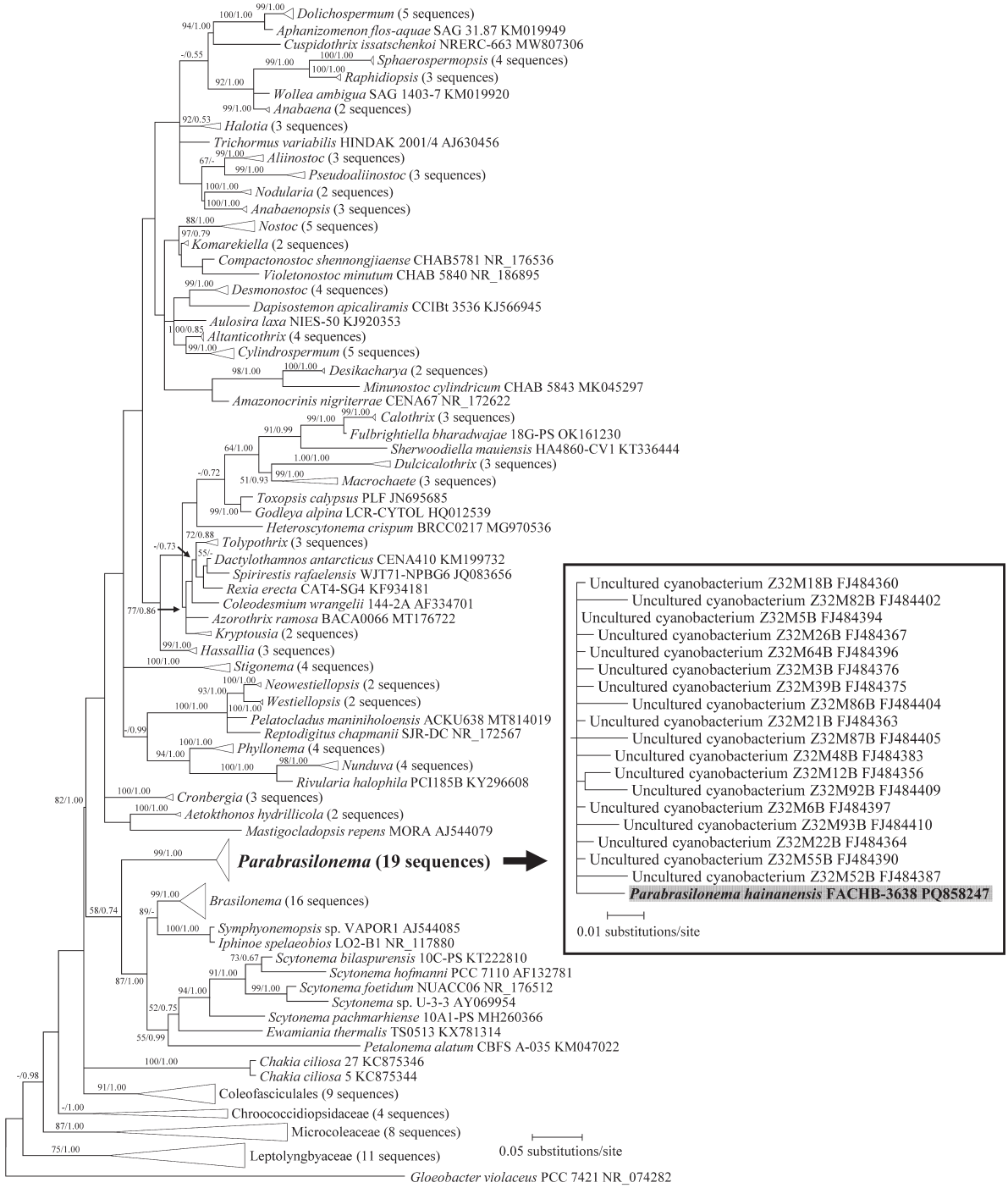

Fig. 4. Maximum likelihood phylogenetic tree based on 16S rRNA gene. Numbers at nodes represent bootstrap support (BP)/ posterior probabilities (PP) from maximum likelihood and Bayesian inference, respectively. Only values of $BP \geq 50\%$ and $PP \geq 0.50$ are shown. The sequence obtained from our study is highlighted in light grey background.

basal heterocytes, wide lamellated sheaths and false branching adjacent to heterocytes or after filament disintegration (Komárek & Johansen, 2015). Genera like *Scytonema*, *Scytonematopsis* and *Chakia* exhibit richly and repeatedly branched thalli. However, *Chakia* forms both typically heteropolar simple filaments and repeated tolypotrichoid branching (Komárková *et al*., 2013). *Iningainema* resembles *Scytonematopsis* and *Scytonema* morphologically but is distinguished by its irregularly spherical to discoid colony formation, broader main filaments, and lateral bulging due to tightly contorted filaments (McGregor & Sendall, 2017a).

Parabrasilonema shares high morphological similarity with *Brasilonema*, *Ewamiania* and *Scytonema*. All four genera possess isopolar filaments enveloped by firm, often layered and colored sheaths (McGregor & Sendall, 2017b). However, unlike *Ewamiania* and *Scytonema*, the genera *Brasilonema* and *Parabrasilonema* exhibit

Table 1. 16S rRNA gene sequence similarities between *Parabrasilonema hainanensis* FACHB–3638 and its closely related taxa.

Strain	1	2	3	4	5	6	7	8	9	10	11	12	13
1. *Parabrasilonema hainanensis* PQ858247													
2. *Cronbergia amazonensis* MF002129	93.89												
3. *Brasilonema angustatum* NR_125582	93.83	93.97											
4. *Brasilonema geniculatum* MG674086	93.20	93.58	98.84										
5. *Brasilonema bromeliae* NR_115807	93.13	93.59	97.07	96.99									
6. *Symphyonemopsis* sp. AJ544085	93.56	94.21	96.14	95.97	96.38								
7. *Iphinoe spelaeobios* NR_117880	92.97	93.75	95.91	95.75	95.98	99.20							
8. *Aetokthonos hydrillicola* KF934176	92.39	95.41	94.41	94.13	93.58	94.12	93.49						
9. *Ewamiania thermalis* KX781314	92.35	92.58	94.28	94.43	94.13	94.37	94.20	93.02					
10. *Chakia ciliosa* KC875346	92.04	91.96	92.36	92.51	91.73	91.88	91.88	91.27	92.04				
11. *Petalonema alatum* KM047022	91.96	90.82	93.18	92.98	92.80	92.13	91.96	90.84	92.51	90.72			
12. *Scytonema foetidum* NR_176512	92.28	92.20	93.36	93.05	92.90	93.00	92.59	92.58	92.74	90.78	91.50		
13. *Scytonema hofmanni* AF132781	91.20	92.36	92.98	93.13	93.21	93.48	93.36	93.22	92.27	90.46	92.80	96.07	
14. Uncultured cyanobacterium Z32M (18 OTUs)	97.51–99.28	93.37–94.75	93.21–94.03	92.81–93.63	92.65–93.47	93.15–93.96	93.28–94.27	93.12–93.91	92.03–92.91	91.61–92.69	91.24–92.80	92.03–92.84	91.24–92.04

macroscopic filaments rarely with or nearly absent false branching (Bohunická *et al*., 2024; Fiore *et al*., 2007). In *Ewamiania*, *Scytonema* and *Brasilonema*, false branching may occur as either geminate or single–tolypotrichoid (Komárek, 2013), with *Ewamiania* commonly displaying tolypotrichoid branching in both field and cultured material (McGregor & Sendall, 2017b). In contrast, no such branching is observed in *Parabrasilonema*. These genera form colonies with erect, densely arranged filaments, sometimes forming fascicles. However, *Ewamiania* and *Parabrasilonema* more commonly exhibit caespitose rather than strictly fasciculate filaments (Fiore *et al*., 2007; McGregor & Sendall, 2017b). The ultrastructure of *Parabrasilonema* aligns with other members of Scytonemataceae, particularly in the arrangement of thylakoids, sheath structure, and the positions of the nucleoplasma and carboxysomes. Notably, the presence of vacuole–like structures, a diagnostic morphological characteristic of *Brasilonema* (Bohunická *et al*., 2024), is also commonly observed in *Parabrasilonema*, particularly large, solitary, central vacuole–like structures in rows of cells (Fiore *et al*., 2007).

Habitat specificity is a valuable taxonomic characteristic for cyanobacteria (Dadheech *et al*., 2012; Řeháková *et al*., 2007). Most members of Scytonemataceae are found in benthic, subaerial, or terrestrial environments, rarely as free–floating plankton (Komárek *et al*., 2010). Many *Scytonema* species are aerial or subaerial on wet rocks, wood and soil, predominantly in tropical regions, while others inhabit periphyton in lakes and coastal waters (Komárek & Johansen, 2015). *Iningainema* species are associated with periphyton in spring waters, subaerial and terrestrial crusts from walls and soils in warm tropical regions (Maltsev *et al*., 2021). The genera *Iphinoe* and *Loriellopsis* are found attached to rocks in European caves (Lamprinou *et al*., 2011), while *Ewamiania* is described from wet mound surface in an Australian thermal spring complex (McGregor & Sendall, 2017b). *Chakia* occurs in algal mats on the bottom of oligotrophic alkaline marshes in tropical and subtropical regions (Komárková *et al*., 2013). *Brasilonema* is commonly found in subaerophytic habitats, attached to substrates such as on tree barks, leaves, stones, walls and moist soil, particularly in humid tropical and subtropical regions (Bohunická *et al*., 2024). *Parabrasilonema* was found in tropical regions, firmly adhering to submerged concrete substrata. Our strain shows a close genetic relationship with 18 sequences of uncultured cyanobacterium, suggesting these may represent previously undescribed *Parabrasilonema* species. Sahl *et al*. (2017) explored Zacatón, a deep (~ 318 m), limestone, phreatic sinkhole in northeastern Mexico and collected biological samples across a vertical gradient, ranging from the water surface to 273 m depth. Notably, these uncultured cyanobacteria were retrieved from wall biomats located at 32m depth within the sinkhole, indicating that *Parabrasilonema* appears capable of thriving in deep and dark environment.

Acknowlegements

This work was supported by National Natural Science Foundation of China (52030002) and National Key R&D Program of China (2020YFA0908801, 2018YFE0110600). We thank Zhenfei Xing and Yuan Xiao at R&D Division of Public Technology and Service, Institute of Hydrobiology, Chinese Academy of Sciences (IHB, CAS) for their assistance in TEM.

References

Barbosa, M., Berthold, D. E., Lefler, F. W., & Laughinghouse IV, H. D. (2021). Diversity of the genus *Brasilonema* (Nostocales, Cyanobacteria) in plant nurseries of central Florida (USA) with the description of three new

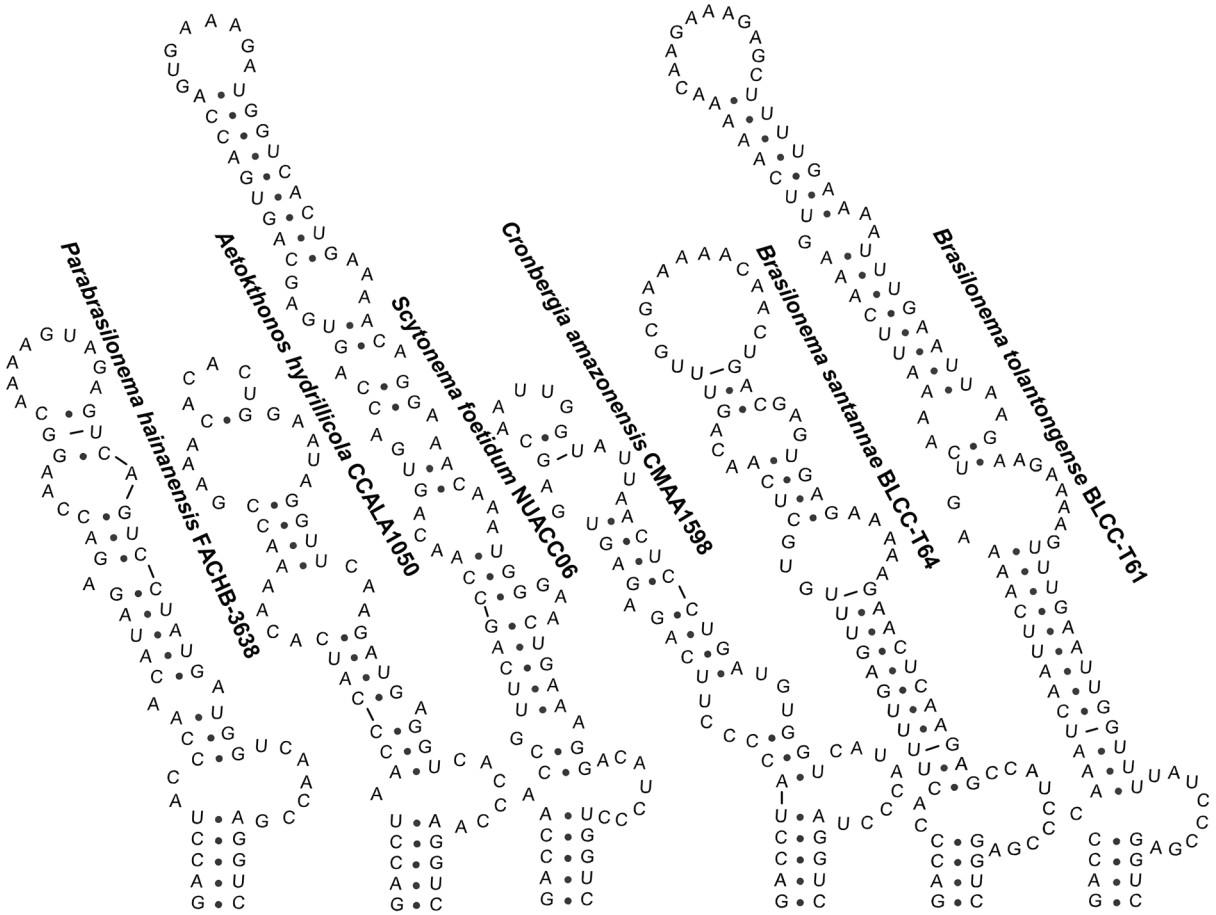

Fig. 5. Predicted secondary structure for D1–D1′ helices of 16S–23S rRNA intergenic spacer sequences from *Parabrasilonema hainanensis* and its related taxa.

species: *B. fioreae* sp. nov., *B. santannae* sp. nov. and *B. wernerae* sp. nov. *Fottea*, *21*, 82–99. https://doi.org/10.5507/fot.2021.006

Baurain, D., Renquin, L., Grubisic, S., Scheldeman, P., Belay, A., & Wilmotte, A. (2002). Remarkable conservation of internally transcribed spacer sequences of *Arthrospira* ("Spirulina") (Cyanophyceae, Cyanobacteria) strains from four continents and of recent and 30-year-old dried samples from Africa. *Journal of Phycology*, *38*(2), 384–393. https://doi.org/10.1046/j.1529-8817.2002.01144.x

Bohunická, M., Johansen, J. R., Villanueva, C. D., Mareš, J., Štenclová, L., Becerra-Absalón, I., Hauer, T., & Kaštovský, J. (2024). Revision of the pantropical genus *Brasilonema* (Nostocales, Cyanobacteria), with the description of 24 species new to science. *Fottea*, *24*, 137–184. https://doi.org/10.5507/fot.2024.006

Castenholz, R. W., & Waterbury, J. B. (1989). Group I. Cyanobacteria. In J. T. Staley, M. P. Bryant, N. Pfennig, & J. G. Holt (Eds.), *Bergey's manual of systematic bacteriology* (Vol. 3, pp. 1710–1728). Williams & Wilkins.

Dadheech, P. K., Mahmoud, H., Kotut, K., & Krienitz, L. (2012). *Haloleptolyngbya alcalis* gen. et sp. nov., a new filamentous cyanobacterium from the soda lake Nakuru, Kenya. *Hydrobiologia*, *691*, 269–283. https://doi.org/10.1007/s10750-012-1085-1

Darriba, D., Taboada, G. L., Doallo, R., & Posada, D. (2012). jModelTest 2: More models, new heuristics and parallel computing. *Nature Methods*, *9*(8), 772. https://doi.org/10.1038/nmeth.2109

Fiore, M. F., Sant'Anna, C. L., Azevedo, M. T. P., Komárek, J., Kaštovský, J., Sulek, J., & Lorenzi, A. S. (2007). The cyanobacterial genus *Brasilonema* gen. nov.: A molecular and phenotypic evaluation. *Journal of Phycology*, *43*(4), 789–798. https://doi.org/10.1111/j.1529-8817.2007.00376.x

Gao, G., Xiao, L., Lin, Q., Hu, R., & Lei, L. (2013). Structure of phytoplankton functional groups and water quality assessment of main reservoirs in Hainan Province. *Ecological Science*, *32*(2), 144–150.

Geitler, L. (1932). *Cyanophyceae*. In L. Rabenhorst (Ed.), *Kryptogamen-Flora von Deutschland, Österreich und der Schweiz* (2nd ed., Vol. 14, pp. 673–1196). Akademische Verlagsgesellschaft.

Iteman, I., Rippka, R., Tandeau de Marsac, N., & Herdman, M. (2000). Comparison of conserved structural and regulatory domains within divergent 16S rRNA–23S rRNA spacer sequences of cyanobacteria. *Microbiology*, *146*(6), 1275–1286. https://doi.org/10.1099/00221287-146-6-1275

Komárek, J. (2013). Phenotypic and ecological diversity of freshwater coccoid cyanobacteria from maritime Antarctica and islands of NW Weddell Sea. I. Synechococcales. *Czech Polar Reports*, *3*(2), 130–143.

Komárek, J., & Johansen, J. R. (2015). Filamentous cyanobacteria. In J. D. Wehr, R. G. Sheath, & J. P. Kociolek (Eds.), *Freshwater algae of North America* (2nd ed., pp. 135–235). Academic Press. https://doi.org/10.1016/B978-0-12-385876-4.00005-5

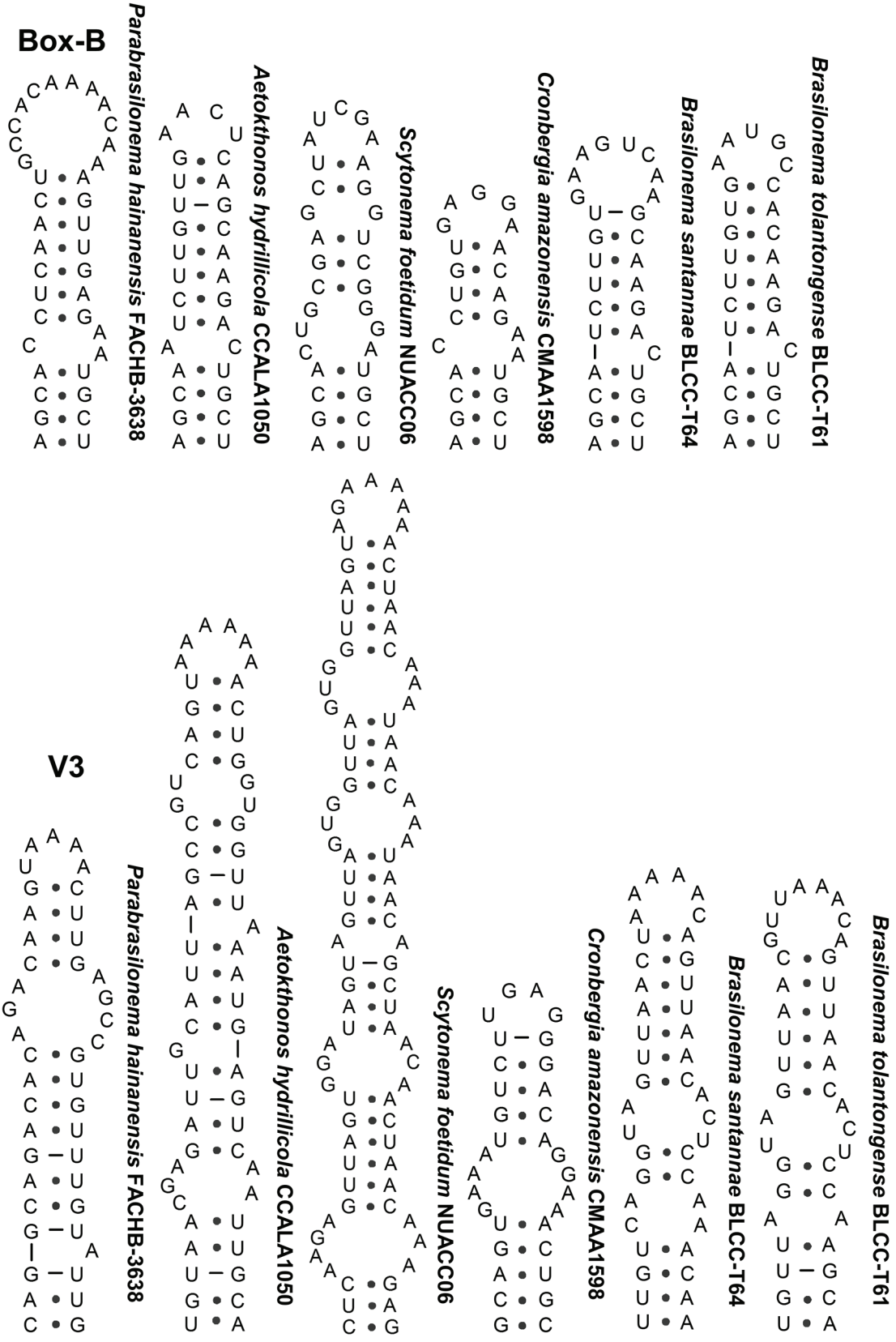

Fig. 6. Predicted secondary structure for Box–B and V3 helices of 16S–23S rRNA intergenic spacer sequences from *Parabrasilonema hainanensis* and its related taxa.

Komárek, J., Kaštovský, J., Mareš, J., & Johansen, J. R. (2014). Taxonomic classification of cyanoprokaryotes (cyanobacterial genera) using a polyphasic approach. *Preslia*, *86*, 295–335.

Komárek, J., Zapomělová, E., & Hindák, F. (2010). *Cronbergia* gen. nov., a new cyanobacterial genus (Cyanophyta) with a special strategy of heterocyte formation. *Cryptogamie, Algologie*, *31*(3), 321–341.

Komárková, J., Zapomělová, E., & Komárek, J. (2013). *Chakia* (Cyanobacteria), a new heterocytous genus from Belizean marshes identified on the basis of the 16S rRNA gene. *Fottea*, *13*(2), 227–233.

Kumar, N., Saraf, A., Pal, S., Mishra, D., Singh, P., & Johansen, J. R. (2023). Circumscription of *Fulbrightiella* gen. nov. and *Sherwoodiella* gen. nov., two novel genera in the Calotrichaceae (Nostocales, Cyanobacteria). *Journal of Phycology*, *59*(1), 204–220. https://doi.org/10.1111/jpy.13341

Kumar, S., Stecher, G., Li, M., Knyaz, C., & Tamura, K. (2018). MEGA X: Molecular evolutionary genetics analysis across computing platforms. *Molecular Biology and Evolution*, *35*(6), 1547–1549. https://doi.org/10.1093/molbev/msy096

Lamprinou, V., Christodoulou, M., Hernández-Mariné, M., Parmakelis, A., & Economou-Amilli, A. (2016). *Spelaeonaias* gen. nov., a new true-branched cyanobacterium from Cave Vlychada (Diros, Peloponnese, Greece). *Phytotaxa*, *282*(3), 171–185. https://doi.org/10.11646/phytotaxa.282.3.1

Lamprinou, V., Hernández-Mariné, M., Canals, T., Kormas, K., Economou-Amilli, A., & Pantazidou, A. (2011). Morphology and molecular evaluation of *Iphinoe spelaeobios* gen. nov., sp. nov. and *Loriellopsis cavernicola* gen. nov., sp. nov. *International Journal of Systematic and Evolutionary Microbiology*, *61*(11), 2907–2915. https://doi.org/10.1099/ijs.0.028787-0

Larkin, M. A., Blackshields, G., Brown, N. P., Chenna, R., McGettigan, P. A., McWilliam, H., … Higgins, D. G. (2007). Clustal W and Clustal X version 2.0. *Bioinformatics*, *23*(21), 2947–2948. https://doi.org/10.1093/bioinformatics/btm404

Mai, T., Johansen, J. R., Pietrasiak, N., Bohunická, M., & Martin, M. (2018). Revision of the Synechococcales (Cyanobacteria) through recognition of four families including Oculatellaceae fam. nov. and Trichocoleaceae fam. nov. and six new genera containing 14 species. *Phytotaxa*, *365*(1), 1–59. https://doi.org/10.11646/phytotaxa.365.1.1

Maltsev, Y., Kezlya, E., Maltseva, S., Karthick, B., & Dvořák, P. (2021). A new species of the previously monotypic genus *Iningainema* (Cyanobacteria, Scytonemataceae) from the Western Ghats, India. *European Journal of Phycology*, *56*(3), 348–358. https://doi.org/10.1080/09670262.2020.1858095

Mareš, J. (2017). Multilocus and SSU rRNA gene phylogenetic analyses of available cyanobacterial genomes, and their relation to the current taxonomic system. *Hydrobiologia*, *811*, 19–34. https://doi.org/10.1007/s10750-017-3370-2

McGregor, G. B., & Sendall, B. C. (2017a). *Iningainema pulvinus* gen. nov., sp. nov. (Cyanobacteria, Scytonemataceae), a new nodularin producer from Edgbaston Reserve, north-eastern Australia. *Harmful Algae*, *62*, 10–19. https://doi.org/10.1016/j.hal.2016.11.006

McGregor, G. B., & Sendall, B. C. (2017b). *Ewamiania thermalis* gen. et sp. nov. (Cyanobacteria, Scytonemataceae), a new cyanobacterium from Talaroo thermal springs, north-eastern Australia. *Australian Systematic Botany*, *30*(1), 38–47. https://doi.org/10.1071/SB16024

Nübel, U., Garcia-Pichel, F., & Muyzer, G. (1997). PCR primers to amplify 16S rRNA genes from cyanobacteria. *Applied and Environmental Microbiology*, *63*(8), 3327–3332.

Řeháková, K., Johansen, J. R., Casamatta, D. A., Li, X., & Vincent, J. (2007). Morphological and molecular characterization of selected desert soil cyanobacteria: Three species new to science including *Mojavia pulchra* gen. et sp. nov. *Phycologia*, *46*(5), 481–502. https://doi.org/10.2216/06-86.1

Ronquist, F., Teslenko, M., Van der Mark, P., Ayres, D. L., Darling, A., Höhna, S., … Huelsenbeck, J. P. (2012). MrBayes 3.2: Efficient Bayesian phylogenetic inference and model choice across a large model space. *Systematic Biology*, *61*(3), 539–542. https://doi.org/10.1093/sysbio/sys029

Sahl, J. W., Fairfield, N., Harris, J. K., Wettergreen, D., Stone, W. C., & Spear, J. R. (2010). Novel microbial diversity retrieved by autonomous robotic exploration of the world's deepest vertical phreatic sinkhole. *Astrobiology*, *10*(2), 201–213. https://doi.org/10.1089/ast.2009.0379

Spurr, A. R. (1969). A low-viscosity epoxy resin embedding medium for electron microscopy. *Journal of Ultrastructure Research*, *26*(1–2), 31–43. https://doi.org/10.1016/S0022-5320(69)90033-1

Stanier, R. Y., Kunisawa, R., & Mandel, M. (1971). Purification and properties of unicellular blue-green algae. *Bacteriological Reviews*, *35*(2), 171–205.

Strunecký, O., Ivanova, A. P., & Mareš, J. (2023). An updated classification of cyanobacterial orders and families based on phylogenomic and polyphasic analysis. *Journal of Phycology*, *59*(1), 12–51. https://doi.org/10.1111/jpy.13317

Whitton, B. A., & Potts, M. (2012). Introduction to the cyanobacteria. In B. A. Whitton & M. Potts (Eds.), *Ecology of cyanobacteria II: Their diversity in space and time* (pp. 1–13). Springer. https://doi.org/10.1007/978-94-007-3855-3_1

Wilde, S. B., Johansen, J. R., Wilde, H. D., Jiang, P., Bartelme, B. A., & Haynie, R. S. (2014). *Aetokthonos hydrillicola* gen. et sp. nov.: Epiphytic cyanobacteria on invasive aquatic plants implicated in avian vacuolar myelinopathy. *Phytotaxa*, *181*(4), 243–260. https://doi.org/10.11646/phytotaxa.181.4.1

Yarza, P., Yilmaz, P., Pruesse, E., Glöckner, F. O., Ludwig, W., Schleifer, K.-H., … Rosselló-Móra, R. (2014). Uniting the classification of cultured and uncultured bacteria and archaea using 16S rRNA gene sequences. *Nature Reviews Microbiology*, *12*(9), 635–645. https://doi.org/10.1038/nrmicro3330

Zhang, Q., Li, L., Yang, Z., Li, T., Zheng, L., & Song, L. (2024). *Limnothece alkaliphila* gen. et sp. nov. (Chroococcales, Cyanobacteria) from an alkaline lake in the Mongolia Plateau, China. *Fottea*, *24*, 232–243. https://doi.org/10.5507/fot.2024.014

Zuker, M. (2003). Mfold web server for nucleic acid folding and hybridization prediction. *Nucleic Acids Research*, *31*(13), 3406–3415. https://doi.org/10.1093/nar/gkg595